Free-Space Quantum Communication with a Portable Quantum Memory

Mehdi Namazi,[1] Giuseppe Vallone,[2] Bertus Jordaan,[1] Connor Goham,[1] Reihaneh Shahrokhshahi,[1] Paolo Villoresi,[2] and Eden Figueroa[1]

[1]*Department of Physics and Astronomy, Stony Brook University, New York 11794-3800, USA*
[2]*Department of Information Engineering, University of Padova, Via Gradenigo 6b, 35131 Padova, Italy*

(Received 27 September 2016; revised manuscript received 17 October 2017; published 14 December 2017)

The realization of an elementary quantum network that is intrinsically secure and operates over long distances requires the interconnection of several quantum modules performing different tasks. In this work, we report the realization of a communication network functioning in a quantum regime, consisting of four different quantum modules: (i) a random polarization qubit generator, (ii) a free-space quantum-communication channel, (iii) an ultralow-noise portable quantum memory, and (iv) a qubit decoder, in a functional elementary quantum network possessing all capabilities needed for quantum-information distribution protocols. We create weak coherent pulses at the single-photon level encoding polarization states $|H\rangle$, $|V\rangle$, $|D\rangle$, and $|A\rangle$ in a randomized sequence. The random qubits are sent over a free-space link and coupled into a dual-rail room-temperature quantum memory and after storage and retrieval are analyzed in a four-detector polarization analysis akin to the requirements of the BB84 protocol. We also show ultralow noise and fully portable operation, paving the way towards memory-assisted all-environment free-space quantum cryptographic networks.

DOI: 10.1103/PhysRevApplied.8.064013

I. INTRODUCTION

The field of quantum information has recently seen remarkable progress regarding the implementation of elementary quantum devices and quantum-communication protocols. On one hand, the advent of photonic quantum communication using long-distance free-space links [1–5] has opened possibilities to securely exchange quantum states and entanglement [6–8]. These developments together with quantum key distribution (QKD) protocols have enormous potential for the creation of a global, secure quantum-information exchange network [9–15]. On the other hand, an entirely different community of quantum scientists has developed sophisticated quantum light matter interfaces capable of receiving, storing, and retrieving photonic qubits [16–19]. Such devices, collectively known as quantum memories, already operate with high fidelities [20–22], long storage times [23,24], and high storage efficiencies [25,26]. Furthermore, quantum memories already operate at room temperature [27–29], thus facilitating their interconnection with other quantum devices.

The construction of an interconnected set of many quantum devices that performs secure communication protocols in outside settings and with moving targets is now within experimental reach [30–32]. Therefore, it is of utmost relevance to engineer elementary networks of a few quantum nodes and quantum channels in order to understand the potential of these architectures [33–36]. The emergent behavior of such small quantum networks should allow us to realize more sophisticated quantum procedures [37]. An important example of such an elementary network will be the modular connection of quantum-cryptography systems operating over free-space quantum channels [38], assisted by room-temperature quantum memories increasing the distance, security, and connectivity of quantum key distribution protocols [14,15].

Paramount to the creation of such a free-space memory-assisted quantum-communication network is the use of shot-by-shot unconditional quantum memories capable of supporting the specific technical demands of outside-of-the-laboratory quantum-communication channels. Among them are accepting random qubit states necessary to perform quantum key distribution protocols, having a minimized quantum bit error rate (QBER), and receiving spatially multimode signals, while simultaneously being cost effective and fully portable. These capabilities will allow the construction of elementary quantum networks without the need for frequency conversion among their components, that are intrinsically secure, quantum coherent, and compatible with long-distance operation.

Here we report the creation of such an elementary quantum network in which we mimic these desired properties into a scaled-down setup. We present individual experiments addressing the various challenges in order to create the quantum connectivity needed to perform memory-assisted long-distance communication of random polarization qubits. Our results represent the ideas of quantum communication, as used in the well-known BB84 protocol, combined with low-noise room-temperature quantum storage. Our results are obtained by cascading four different quantum modules: a random polarization qubit generator, a free-space quantum-communication channel, warm vapor quantum memory, and a qubit decoder.

II. EXPERIMENTAL PROCEDURE

A. Preparation of a random stream of qubits: Alice's module

Our elementary quantum network starts with the creation of a sequence of four polarization states $[|H\rangle, |V\rangle, |D\rangle = 1/\sqrt{2}(|H\rangle + |V\rangle), |A\rangle = 1/\sqrt{2}(|H\rangle - |V\rangle)]$ in a distant laboratory (Alice's station, laboratory II in Fig. 1). We create the qubits using 400-ns-long pulses produced every 40 μs by four individual acousto-optical modulators (AOMs). In order to compensate for small deviations in the length of each AOM track, the AOMs are each driven by independent sources regarding their amplitude and frequency modulation. The setup is designed to generate either an ordered sequence of four qubits in cycles of 160 μs (see Fig. 2) or a train of qubit pulses where the modulation sources are controlled by a field-programmable gate array chip programed to randomly trigger one of the four AOMs. The resulting random sequence of pulses is attenuated to the single-photon level and then sent into a free-space quantum channel module.

B. Propagation of qubit streams: Free-space quantum channel module

The qubits created in the Alice station propagate in a free-space quantum-communication channel over a distance of approximately 20 m without shielding or vacuum propagation and are then directed to a quantum-memory setup in a different laboratory. We choose the characteristics of this setup as a test bed of the interconnectivity of this station and the quantum-memory setup under more challenging out-of-the-laboratory operation. Of particular interest are the shot-by-shot changes in the mean input photon number due to the air turbulence between the laboratories and the capability of the memory to receive random polarization inputs, pulse by pulse. By careful alignment, the loss in the free-space propagation is set to be less than 4%. Together with 63% fiber coupling efficiency at the receiving end of the quantum-memory setup, this yields a total transmission of 59% for the quantum-communication channel. The shot-by-shot fluctuations in the mean photon number are measured to be approximately 5%.

C. Storage of incoming pulses: Quantum-memory module

Located in laboratory I is the room-temperature quantum memory in which we store the incoming qubits. The quantum memory is based upon a warm ^{87}Rb vapor and controlled using electromagnetically induced transparency (EIT). Two independent control beams coherently prepare two volumes within a single ^{87}Rb vapor cell at 60 °C, containing Kr buffer gas to serve as the storage medium for each mode of the polarization qubit. We employ two external-cavity diode lasers phase locked at 6.835 GHz. The probe-field frequency is stabilized to the $5S_{1/2}F = 1 \rightarrow 5P_{1/2}F' = 1$ transition at a wavelength of 795 nm, while the control field interacts with the $5S_{1/2}F = 2 \rightarrow 5P_{1/2}F' = 1$ transition. Polarization elements supply 42 dB of control-field attenuation (80% probe transmission), while two temperature-controlled etalon resonators (linewidths of 40 and 24 MHz) provide an additional 102 dB of control-field extinction. The total probe-field transmission is 4.5% for all polarization inputs, exhibiting an effective, control or probe suppression ratio of 130 dB [27]. The control-field pulses are time optimized to the arrival of the qubits in front of the memory [see Fig. 2(a)].

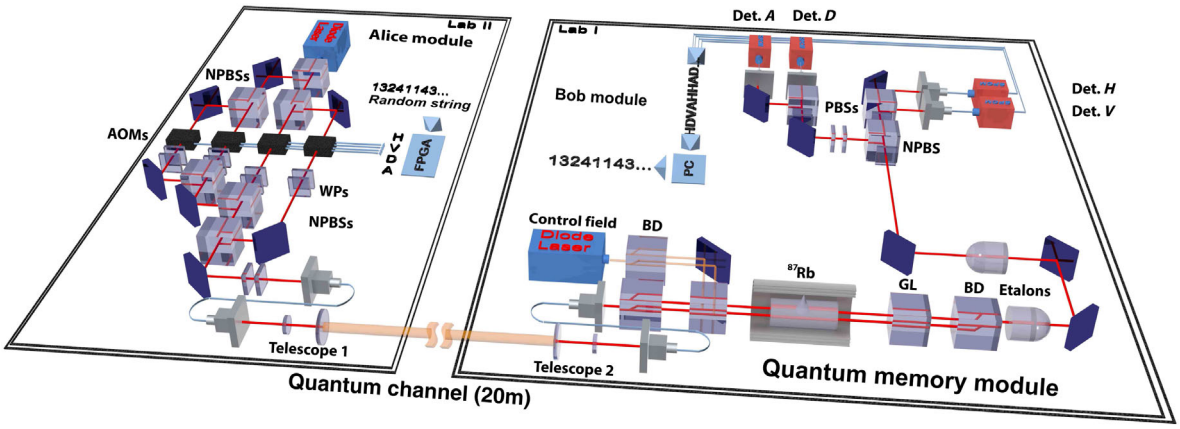

FIG. 1. Experimental setup for free-space quantum communication. In laboratory II, Alice creates a random sequence of four orthogonal qubits ($|H\rangle, |V\rangle, |D\rangle, |A\rangle$). The 400-ns-long qubits are produced every 40 μs. The qubits propagate in a free-space quantum-communication channel over a distance of approximately 20 m and are then directed into a dual-rail room-temperature rubidium vapor quantum memory in laboratory I. The control storage pulses are time optimized to the arrival of the qubits in front of the memory. In Bob's site, a four-detector setup measures all possible bases at the exit of the memory to determine the quantum bit error rate (QBER). PBS, polarizing beam splitter; WP, wave plates; AOM, acousto-optical modulator; BD, beam displacer; GL, Glan-laser polarizer.

D. Measuring the random stream of qubits: Bob's module

After passing through the polarization-independent frequency-filtering system, the stored pulses enter Bob's module, which is equipped with a nonpolarizing beam splitter (separating the $Z = \{|H\rangle, |V\rangle\}$ and $X = \{|D\rangle, |A\rangle\}$ bases) and two polarizing beam splitters whose outputs are detected by four single-photon-counting modules (SPCMs). Each SPCM corresponds to a different polarization state. This allows us to compare the detected sequence with the originally sent qubits and estimate the influence of the photonic background of the memory in the evaluation of the QBERs.

III. EXPERIMENT 1: STORAGE OF A SEQUENCE OF FOUR POLARIZATION QUBITS AFTER FREE-SPACE PROPAGATION

In our first experiment, a string of four ordered polarization qubits ($|H\rangle$, $|V\rangle$, $|D\rangle$, and $|A\rangle$) is sent from Alice's module to the memory and Bob's terminal through the free-space channel in order to test the compatibility of all the modules and the performance of the quantum memory at the single-photon level (see Fig. 2). The characterizations of the qubits after storage is done with a single detector placed after the memory bypassing the polarization analysis setup. We create histograms using the time of arrival and estimate a best-case-scenario fidelity of the stored polarization qubits containing on average 1.6 photons per pulse right before the memory.

We evaluate the signal-to-background ratio (SBR) in the measurements, defined as η/q, where η is the retrieved fraction of a single excitation stored in a quantum memory and q the average number of concurrently emitted photons due to background processes. Both are calculated by integrating the retrieved and background signals over 100-ns intervals. The fidelities are then estimated as $F = 1 - \frac{1}{2}(q/\eta)$. Our analysis shows that, even with the additional constraint of shot-by-shot fluctuations in intensity due to free-space propagation and the addition of randomly polarized background photons in the memory, maximum fidelities of 92% for $|H\rangle$, 92% for $|V\rangle$, 90% for $|D\rangle$, and 93% for $|A\rangle$ can still be achieved.

These results are clearly above the classical threshold limit of 85% for the corresponding efficiencies, thus providing the necessary condition of unconditional quantum-memory operation [27]. They also show that our room-temperature quantum-memory implementation operates with the same parameters regardless of the polarization input, a fundamental attribute if the memory were to work as either a synchronization device for quantum-cryptography protocols in which a stream of random qubits is used to distribute a quantum key or as memory for polarization entanglement in a quantum repeater architecture.

IV. EXPERIMENT 2: STORAGE OF A RANDOM SEQUENCE OF POLARIZATION STATES WITH A HIGH PHOTON NUMBER

After showing unconditional memory operation over the free-space network, we now show that the network also operates with high fidelity on a pulse-by-pulse basis, demonstrated by a full polarization analysis at Bob's location. This is done by randomizing the polarization input of the experiment. Further insight into our current capabilities is obtained by analyzing the QBERs Q_X and Q_Z for X and Z bases after propagation and storage. Starting with pulses containing a high number of photons (approximately 100 photons; see Fig. 3), we evaluated the QBER after storage of the random polarization states. An average QBER of 0.57% for the two orthogonal bases has been measured within a region of interest equal to the input pulse width. This QBER is compatible with the typical error rate obtained in a standard quantum key

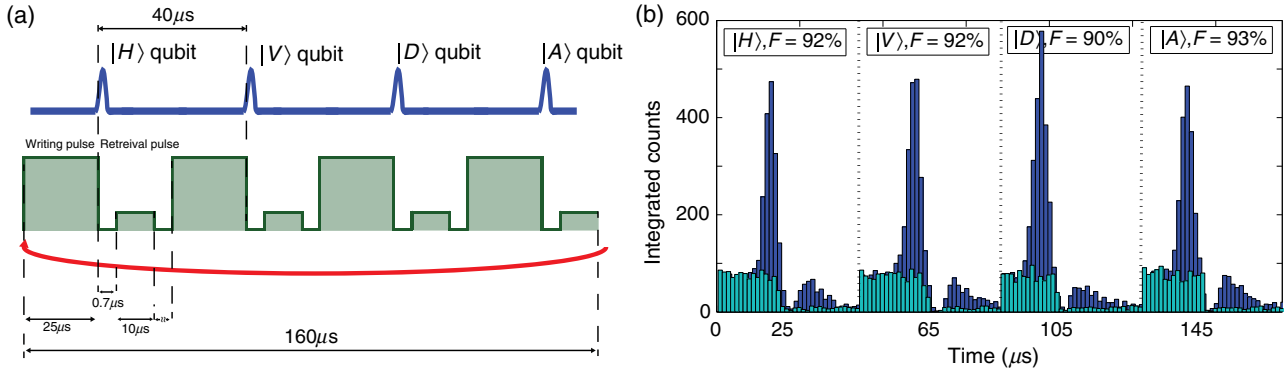

FIG. 2. Storage of a sequence of qubits. (a) A stream of polarization qubits with on average 3.5 photons propagates through a free-space quantum-communication channel of 20 m. In the quantum-memory site, the single-photon-level qubits are received and stored sequentially using timed control-field pulses. (b) Histograms for each of the polarization inputs after storage (dark blue) and background floor (light blue). Each histogram is presented in a 2-μs time interval (see dashed black divisions). The fidelities are estimated from the signal-to-background ratio.

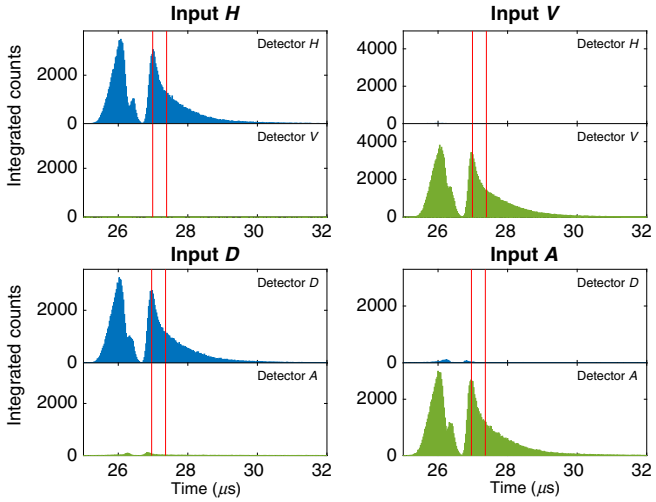

FIG. 3. QBER evaluation of the long-distance communication setup plus memory. In Bob's site, the polarization states are received and stored sequentially in a room-temperature quantum memory. We randomly choose one of the Z and X bases to measure the polarization state and then calculate the QBER over a region of interest equal to the input pulse width (red bars). We show histograms on the photon counts in each of the four polarizations. The first peak represents nonstored photons (leakage), while the second peak represents the retrieved photons. In an experiment with a high-input photon number, the obtained QBERs are less than 1%, as can be seen in the low counts corresponding to undesirable polarization detections.

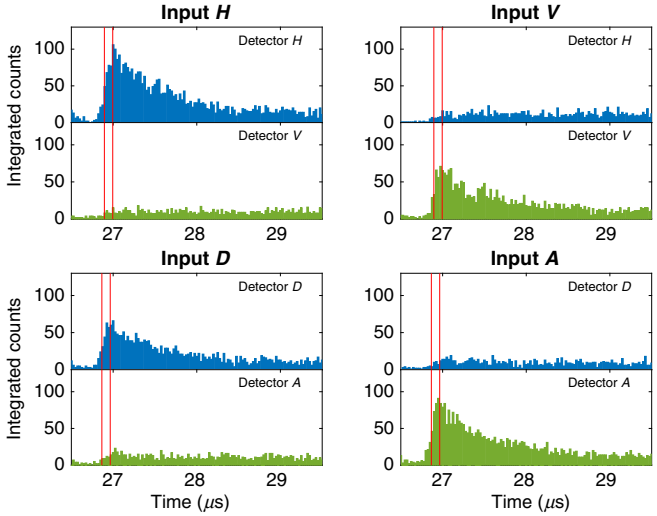

FIG. 4. QBER evaluation for single-photon-level experiment. (a) The QBER is calculated in a 100-ns window (red bars). QBERs of 11.0% and 12.9% are, respectively, achieved for Z and X bases. At the single-photon level, undesirable polarization rotations remain absent, and noise in the orthogonal channel arises from control-field-induced nonlinear processes.

distribution experiment. The importance of this result is twofold: (i) The storage process at room temperature does not intrinsically add nonunitary rotation to the states and in the limit of a high signal-to-background has a negligible effect on the total QBER; (ii) the memory is capable of storing and retrieving generic polarization qubits on a shot-by-shot level.

V. EXPERIMENT 3: STORAGE OF A RANDOM SEQUENCE OF POLARIZATION QUBITS

In our next experiment, the complete state measurement in the two bases is used again for an input of 1.6 photons before the memory, corresponding to 3.5 photons at Alice's station. The evaluated QBERs after storage for polarization qubits are $Q_Z = 11.0\%$ and $Q_X = 12.9\%$ over a 100-ns region (see Fig. 4). The increase of the QBERs is due only to the background noise, which is much more significant at the single-photon level. Nonetheless, the fidelities (corresponding to $F = 1 - \text{QBER}$) still remain higher than the classical limit for the corresponding storage efficiency. The latter result is rather counterintuitive when dealing with superpositions $|D\rangle$ and $|A\rangle$, as it implies that the two rails forming the quantum memory store or miss the pulse coherently (in order to preserve the storage fidelity for that particular polarization), as opposed to retrieving rather $|H\rangle$ or $|V\rangle$ at any given time in a shot-by-shot experiment. This ability is crucial in networks performing quantum key distribution protocols, and it also shows that the memory is currently capable of receiving entangled polarization states without distorting them. We do mention that this last experiment constitutes the quantum-communication part of the well-known BB84 protocol [39], with the addition of a synchronizing quantum memory between Alice and Bob.

VI. EXPERIMENT 4: ULTRALOW-NOISE OPERATION AND QBER IMPROVEMENTS

In order to unlock the potential of our elementary realization as a quantum-cryptography network, the main bottleneck identified in the aforementioned experiments is the memory performance at the required single-photon level. Naturally, there has to exist a compromise between room-temperature, all-environment operation and the background noise of the device at the quantum level, thereby creating limits to the achievable QBER. In our EIT configuration, the single-photon-level background mechanism is produced by several nonlinear effects. Gearing towards increasing the performance of the memory, we perform experiments in which we replace one of the etalons in the filtering system with a similar unit with a different free spectral ratio. This addition limits the background photons created by broad four-wave mixing. To also eliminate the contribution due to incoherent scattering, we also add a weak ($\langle n \rangle \leq 0.01$) auxiliary beam on resonance with the $5S_{1/2}F = 1 \rightarrow 5P_{1/2}F' = 1$ transition that remains on during the complete storage procedure. First results and our interpretation of the data indicate that a total suppression of the background noise can be achieved

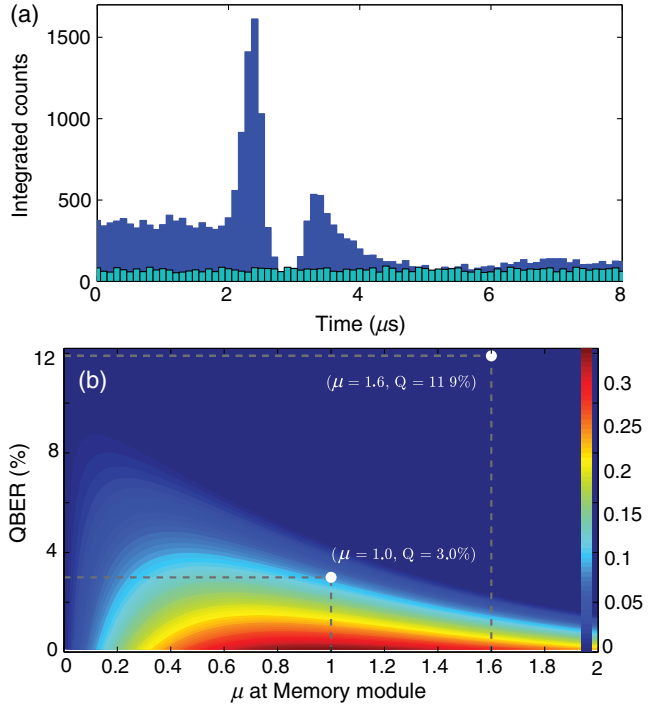

FIG. 5. Ultralow-noise quantum-memory operation. (a) Noise reduction by introducing an auxiliary field; the interaction between dark-state polaritons creates a background-free region. Retrieving the probe under these conditions results in a SBR of >25. The SBR is calculated using a 100-ns integration region at the peak of the retrieve signal and a minimized averaged background obtained in a 1-μs region centered around 5.2 μs (divided by 10). The dark blue histogram includes the signal, background noise, and auxiliary field. The light blue histogram includes only the auxiliary field. (b) Quantum key distribution rate vs mean photon number and quantum bit error rate. The color bar represents the key rate. The line intersecting light blue and dark blue (negative key rate area) corresponds to the boundary for the positive key rate. The white dots indicate the regime of bare quantum memory and ultralow-noise memory regimes.

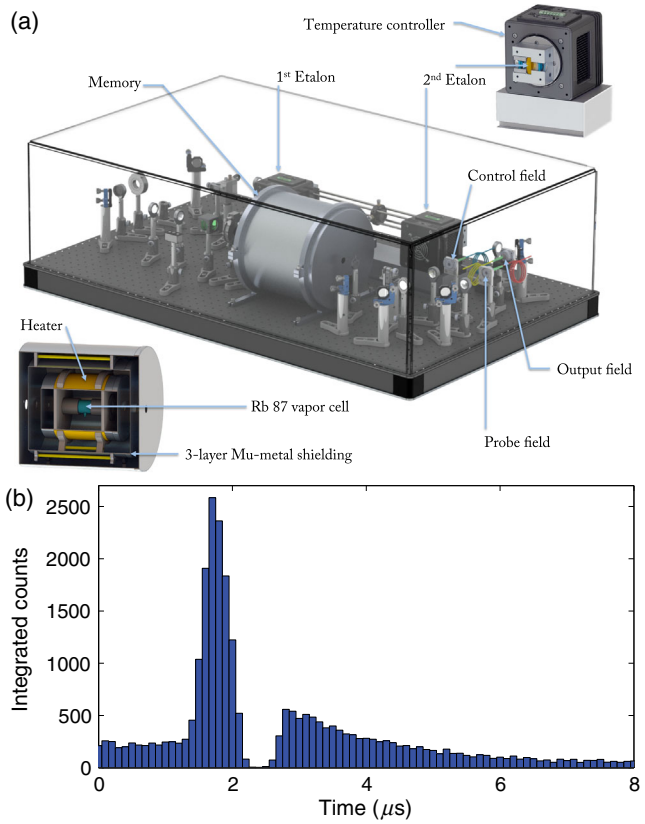

FIG. 6. (a) Prototype of a room-temperature portable quantum memory. Upper-right inset: Detail of one of the frequency filtering units, including the silica etalon, isolation oven, temperature control cold plate, and proportional integral differential temperature-regulation circuitry. Bottom-left inset: Detail of the interaction zone including the Rb cell, temperature control electronics, and three-layer magnetic shielding. (b) Storage of single-photon-level light pulses in the portable quantum memory.

by engineering the interaction of the two created dark-state-polariton modes [40].

Figure 5(a) shows the results of a one-rail experiment including the auxiliary field (light blue). We can see that, after retrieval, the two dark-state-polariton interaction creates regions without the additional background noise. In this experiment, the auxiliary-field strength is increased to highlight the ultralow-noise regions. We measure a SBR of approximately 26 for an input of $\langle n\rangle \sim 1.3$ photons, limited only by the intrinsic attenuation of the filtering system (in contrast to being limited by the background noise). We can then infer a corresponding fidelity of 97% and QBER of approximately 3% for $\langle n\rangle \sim 1$ (see the caption in Fig. 5). Another important consequence of this measurement is the possible increase of the efficiency at the single-photon level, as restrictions on the control-field power used for retrieving are now lifted. This will boost the storage efficiency to 50%.

The relevance of this new regime of operation is highlighted by analyzing its consequences in the achievable quantum key distribution rate (R) per channel efficiency for sharing a random secret key, encoded in random polarization states, between Alice and Bob. R depends on the QBER and the mean photon number μ. In the infinite key length limit, it is given by $R=\mu\{e^{-\mu}[1-H(Q_X)]-H(Q_Z)f(Q_Z)\}$, where Q_X and Q_Z are the QBERs, $H(x)$ is the binary Shannon entropy function, and $f(Q_Z)$ is the efficiency of the classical error-correction protocol. We evaluate the absolute key rate vs the input photon number and our average QBER with $f(Q_Z)=1.05$ [41] for two cases. In the first case, we include the bare quantum-memory operation (QBER $=11.9\%$ for $\mu=1.6$). Figure 5(b) shows that this regime lies just outside of the region for positive key rate generation, indicating not fully secure qubit communication. This situation is fully corrected by applying the noise-reduction techniques explained above, as in this new regime the operation (QBER $=3\%$ for $\mu=1$) is well inside the secure communication threshold. This is a very important achievement, as our quantum network has all the elementary capabilities for quantum-cryptography operation.

VII. EXPERIMENT 5: FULLY PORTABLE QUANTUM-MEMORY OPERATION

In order to boost the achieved quantum network operation towards all-environment qubit connections between distant isolated locations, portable and robust quantum memories are paramount. In our last experiment, we show the storage of single-photon-level qubits in a prototype of a fully portable plug-and-play memory. This prototype has the same features of the designs used in our aforementioned experiments but is fully independent of laboratory infrastructure, as it requires only the probe photons and an EIT control field as inputs. It also possesses a miniaturized version of the filtering system with independent temperature controllers. This device has already proven to be fully portable, as it was built in Stony Brook University and shipped to the Royal Institute of Technology in Stockholm. There it has been shown to be fully operational and easily integrated with independent quantum light sources. These experimental results will be published elsewhere. A detailed depiction of the portable memory is shown in Fig. 6(a). In Fig. 6(b), we show a storage-of-light experiment in which we store pulses with a mean photon number $\langle n \rangle \sim 2$, in a single-rail experiment, corresponding to a SBR of 7.2.

VIII. CONCLUSIONS

In conclusion, we show a network of quantum devices in which breakthrough operational capabilities are possible. We achieve the proof-of-principle combination of free-space propagation of random single-photon-level polarization qubits and their storage and retrieval in a room-temperature quantum memory. These results effectively constitute the quantum part of the BB84 protocol with the addition of a quantum memory. Furthermore, we show noise-suppression techniques that allow our network to operate in a regime useful for quantum-cryptographic communication with low QBERs. Last, we show fully portable room-temperature quantum-memory operation. Together, all these capabilities pave the way for more sophisticated applications using a network of portable quantum memories.

Because free-space propagation does not require the challenge of frequency conversion to the infrared, our setup can already be used for short-distance proof-of-concept memory-assisted device-independent QKD experiments. For example, performing Hong-Ou-Mandel (HOM) photon interference using photons retrieved from two memories, together with memory-assisted temporal shaping of the outgoing qubits [42–44] and applying the aforementioned noise-reduction techniques, will make it possible to store two random streams of qubits independently in each memory and to perform Bell measurements after simultaneous retrieval events. We also envision that the portable aspect of the memories will allow their use in remote observatory locations, opening a pathway for experiments with photons traveling over ultralong satellite communication channels. The performance of our envisioned applications will benefit by a continuous development of our portable technology, including an increase in the speed (bandwidth) of the memory together with a shorter pulse duration and an increase in the success rate of the storage procedure by means of heralding.

ACKNOWLEDGMENTS

We thank Ruoxi Wang and Mael Flament for technical assistance in the development of the portable quantum-memory setup. The work is supported by the U.S. Navy Office of Naval Research, Grant No. N00141410801, the National Science Foundation, Grant No. PHY-1404398, and the Simons Foundation, Grant No. SBF241180. B. J. acknowledges financial assistance of the National Research Foundation (NRF) of South Africa.

[1] I. Capraro, A. Tomaello, A. Dall'Arche, F. Gerlin, R. Ursin, G. Vallone, and P. Villoresi, Impact of Turbulence in Long Range Quantum and Classical Communications, Phys. Rev. Lett. **109**, 200502 (2012).

[2] G. Vallone, V. D'Ambrosio, A. Sponselli, S. Slussarenko, L. Marrucci, F. Sciarrino, and P. Villoresi, Free-Space Quantum Key Distribution by Rotation-Invariant Twisted Photons, Phys. Rev. Lett. **113**, 060503 (2014).

[3] G. Vallone, D. Bacco, D. Dequal, S. Gaiarin, V. Luceri, G. Bianco, and P. Villoresi, Experimental Satellite Quantum Communications, Phys. Rev. Lett. **115**, 040502 (2015).

[4] T. Schmitt-Manderbach, H. Weier, M. Fürst, R. Ursin, F. Tiefenbacher, T. Scheidl, J. Perdigues, Z. Sodnik, C. Kurtsiefer, J. G. Rarity, A. Zeilinger, and H. Weinfurter, Experimental Demonstration of Free-Space Decoy-State Quantum Key Distribution over 144 km, Phys. Rev. Lett. **98**, 010504 (2007).

[5] S. Nauerth, F. Moll, M. Rau, C. Fuchs, J. Horwath, S. Frick, and H. Weinfurter, Air-to-ground quantum communication, Nat. Photonics **7**, 382 (2013).

[6] S. Ritter, C. Nölleke, C. Hahn, A. Reiserer, A. Neuzner, M. Uphoff, M. Mücke, E. Figueroa, J. Bochmann, and G. Rempe, An elementary quantum network of single atoms in optical cavities, Nature (London) **484**, 195 (2012).

[7] K. S. Choi, A. Goban, S. B. Papp, S. J. van Enk, and H. J. Kimble, Entanglement of spin waves among four quantum memories, Nature (London) **468**, 412 (2010).

[8] C. Nölleke, A. Neuzner, A. Reiserer, C. Hahn, G. Rempe, and S. Ritter, Efficient Teleportation between Remote Single-Atom Quantum Memories, Phys. Rev. Lett. **110**, 140403 (2013).

[9] V. Scarani, H. Bechmann-Pasquinucci, N. J. Cerf, M. Dušek, N. Lütkenhaus, and M. Peev, The security of practical quantum key distribution, Rev. Mod. Phys. **81**, 1301 (2009).

[10] H.-K. Lo, M. Curty, and B. Qi, Measurement-Device-Independent Quantum Key Distribution, Phys. Rev. Lett. **108**, 130503 (2012).

[11] D. Bacco, M. Canale, N. Laurenti, G. Vallone, and P. Villoresi, Experimental quantum key distribution with

finite-key security analysis for noisy channels, Nat. Commun. **4**, 2363 (2013).
[12] Y. Liu, T.-Y. Chen, L.-J. Wang, H. Liang, G.-L. Shentu, J. Wang, K. Cui, H.-L. Yin, N.-L. Liu, L. Li, X. Ma, J. S. Pelc, M. M. Fejer, C.-Z. Peng, Q. Zhang, and J.-W. Pan, Experimental Measurement-Device-Independent Quantum Key Distribution, Phys. Rev. Lett. **111**, 130502 (2013).
[13] Z. Tang, Z. Liao, F. Xu, B. Qi, L. Qian, and H.-K. Lo, Experimental Demonstration of Polarization Encoding Measurement-Device-Independent Quantum Key Distribution, Phys. Rev. Lett. **112**, 190503 (2014).
[14] S. Abruzzo, H. Kampermann, and D. Bruß, Measurement-device-independent quantum key distribution with quantum memories, Phys. Rev. A **89**, 012301 (2014).
[15] C. Panayi, M. Razavi, X. Ma, and N. Lütkenhaus, Memory-assisted measurement-device-independent quantum key distribution, New J. Phys. **16**, 043005 (2014).
[16] A. Reiserer and G. Rempe, Cavity-based quantum networks with single atoms and optical photons, Rev. Mod. Phys. **87**, 1379 (2015).
[17] T. E. Northup and R. Blatt, Quantum information transfer using photons, Nat. Photonics **8**, 356 (2014).
[18] F. Bussières, N. Sangouard, M. Afzelius, H. de Riedmatten, C. Simon, and W. Tittel, Prospective applications of optical quantum memories, J. Mod. Opt. **60**, 1519 (2013).
[19] K. Heshami, D. G. England, P. C. Humphreys, P. J. Bustard, V. M. Acosta, J. Nunn, and B. J. Sussman, Quantum memories: Emerging applications and recent advances, J. Mod. Opt. **63**, 2005 (2016).
[20] S. Riedl, M. Lettner, C. Vo, S. Baur, G. Rempe, and S. Dürr, Bose-Einstein condensate as a quantum memory for a photonic polarization qubit, Phys. Rev. A **85**, 022318 (2012).
[21] M. Gündoğan, P. M. Ledingham, A. Almasi, M. Cristiani, and H. de Riedmatten, Quantum Storage of a Photonic Polarization Qubit in a Solid, Phys. Rev. Lett. **108**, 190504 (2012).
[22] E. Saglamyurek, J. Jin, V. B. Verma, M. D. Shaw, F. Marsili, S. W. Nam, D. Oblak, and W. Tittel, Quantum storage of entangled telecom-wavelength photons in an erbium-doped optical fibre, Nat. Photonics **9**, 83 (2015).
[23] I. Novikova, R. Walsworth, and Y. Xiao, Electromagnetically induced transparency-based slow and stored light in warm atoms, Laser Photonics Rev. **6**, 333 (2012).
[24] Y.-F. Hsiao, P.-J. Tsai, H.-S. Chen, S.-X. Lin, C.-C. Hung, C.-H. Lee, Y.-H. Chen, Y.-F. Chen, I. A. Yu, and Y.-C. Chen, EIT-based photonic memory with near-unity storage efficiency, arXiv:1605.08519.
[25] M. Hosseini, B. M. Sparkes, G. Campbell, P. K. Lam, and B. C. Buchler, High efficiency coherent optical memory with warm rubidium vapour, Nat. Commun. **2**, 174 (2011).
[26] S.-J. Yang, X.-J. Wang, X.-H. Bao, and J.-W. Pan, An efficient quantum lightmatter interface with sub-second lifetime, Nat. Photonics **10**, 381 (2016).
[27] M. Namazi, C. Kupchak, B. Jordaan, R. Shahrokhshahi, and E. Figueroa, Ultra-Low-Noise Room-Temperature Quantum Memory for Polarization Qubits, Phys. Rev. Applied **8**, 034023 (2017).
[28] D. G. England, K. A. Fisher, J.-P. W. MacLean, P. J. Bustard, R. Lausten, K. J. Resch, and B. J. Sussman, Storage and Retrieval of THz-Bandwidth Single Photons Using a Room-Temperature Diamond Quantum Memory, Phys. Rev. Lett. **114**, 053602 (2015).
[29] D. Saunders, J. Munns, T. Champion, C. Qiu, K. Kaczmarek, E. Poem, P. Ledingham, I. Walmsley, and J. Nunn, Cavity-Enhanced Room-Temperature Broadband Raman Memory, Phys. Rev. Lett. **116**, 090501 (2016).
[30] *The Physics of Quantum Information*, edited by D. Bouwmeester, A. Ekert, and A. Zeilinger (Springer, Berlin, 2000), ISBN 978-3-642-08607-6.
[31] J. I. Cirac, P. Zoller, H. J. Kimble, and H. Mabuchi, Quantum State Transfer and Entanglement Distribution among Distant Nodes in a Quantum network, Phys. Rev. Lett. **78**, 3221 (1997).
[32] H. J. Kimble, The quantum internet, Nature (London) **453**, 1023 (2008).
[33] A. Datta, L. Zhang, J. Nunn, N. K. Langford, A. Feito, M. B. Plenio, and I. A. Walmsley, Compact Continuous-Variable Entanglement Distillation, Phys. Rev. Lett. **108**, 060502 (2012).
[34] P. Kómár, E. M. Kessler, M. Bishof, L. Jiang, A. S. Sørensen, J. Ye, and M. D. Lukin, A quantum network of clocks, Nat. Phys. **10**, 582 (2014).
[35] A. Reiserer, N. Kalb, M. S. Blok, K. J. M. van Bemmelen, T. H. Taminiau, R. Hanson, D. J. Twitchen, and M. Markham, Robust Quantum-Network Memory Using Decoherence-Protected Subspaces of Nuclear Spins, Phys. Rev. X **6**, 021040 (2016).
[36] F. Bussières, C. Clausen, A. Tiranov, B. Korzh, V. B. Verma, S. W. Nam, F. Marsili, A. Ferrier, P. Goldner, H. Herrmann, C. Silberhorn, W. Sohler, M. Afzelius, and N. Gisin, Quantum teleportation from a telecom-wavelength photon to a solid-state quantum memory, Nat. Photonics **8**, 775 (2014).
[37] L.-M. Duan, M. D. Lukin, J. I. Cirac, and P. Zoller, Long-distance quantum communication with atomic ensembles and linear optics, Nature (London) **414**, 413 (2001).
[38] G. Vallone, D. Dequal, M. Tomasin, F. Vedovato, M. Schiavon, V. Luceri, G. Bianco, and P. Villoresi, Interference at the Single Photon Level along Satellite-Ground Channels, Phys. Rev. Lett. **116**, 253601 (2016).
[39] C. H. Bennett and G. Brassard, in *Proceedings of the IEEE International Conference on Computers, Systems and Signal Processing, Bangalore, India* (IEEE, New York, 1984), p. 175.
[40] L. Karpa, F. Vewinger, and M. Weitz, Resonance Beating of Light Stored Using Atomic Spinor Polaritons, Phys. Rev. Lett. **101**, 170406 (2008).
[41] D. Elkouss, J. Martinez-Mateo, and V. Martin, Information reconciliation for quantum key distribution, Quantum Inf. Comput. **11**, 0226 (2011).
[42] M. Namazi, T. Mittiga, C. Kupchak, and E. Figueroa, Cascading quantum light-matter interfaces with minimal interconnection losses, Phys. Rev. A **92**, 033846 (2015).
[43] P. Farrera, G. Heinze, B. Albrecht, M. Ho, M. Chávez, C. Teo, N. Sangouard, and H. de Riedmatten, Generation of single photons with highly tunable wave shape from a cold atomic ensemble, Nat. Commun. **7**, 13556 (2016).
[44] P. B. R. Nisbet-Jones, J. Dilley, D. Ljunggren, and A. Kuhn, Highly efficient source for indistinguishable single photons of controlled shape, New J. Phys. **13**, 103036 (2011).